Copper complexes from 3,5-disubstituted N-hydroxyethylpyrazole ligands: Cleavage of C–N bond as well as formation of second coordination sphere complexes

Joan Soldevila-Sanmartín [a], Teresa Calvet [b], Mercè Font-Bardia [c], José G. Planas [d], Josefina Pons [a,*]

[a] Departament de Química, Universitat Autònoma de Barcelona, 08913 Bellaterra, Barcelona, Spain

[b] Departament de Mineralogia, Petrologia i Geologia Aplicada, Universitat de Barcelona, Martí i Franquès s/n, 08028 Barcelona, Spain

[c] Unitat de Difracció de Raigs-X, Centres Científics i Tecnològics de la Universitat de Barcelona (CCiTUB), Universitat de Barcelona, Solé i Sabarís, 1-3, 08028 Barcelona, Spain

[d] Institut de Ciència de Materials de Barcelona, ICMAB-CSIC, Campus UAB, 08193Bellaterra, Spain

*** Corresponding author.**

E-mail address: josefina.pons@uab.cat (J. Pons).

Abstract

The coordination behaviour of two N,O-hybrid hydroxyethylpyrazole ligands, 2-(3,5-diphenyl-1H-pyrazol-1-yl) ethanol, HL1; and (2-(3,5-di(2-pyridyl)-1H-pyrazol-1-yl)ethanol, HL2; with CuCl2·2H2O and Cu(NO3)2·3H2O were studied. Four copper complexes: [CuCl(μ-L1)]2·HL1 (1), [CuCl2(HL2)]·H2O (2A), [Cu(NO3)(3,5-hdppz) (μ-L1)]2·2CH3CN (3), (3,5-hdppz = 3,5-diphenylpyrazole) and [Cu(H2O) (3,5-dpypz)]2 (NO3)2·H2O (4), (3,5-dpypz = 3,5-(2-pyridyl) pyrazolate) were isolated and characterized by analytical methods and spectroscopical studies. From their crystal structure, a Npz-C bond cleavage was observed for HL1 and HL2 upon reaction with Cu (NO3)2·3H2O, yielding the unexpected complexes 3 and 4, respectively. Overall, these complexes provided great structural diversity, as dimers (asymmetric and symmetric), monomers and ionic complexes were obtained. Finally, magnetic susceptibility measurements for 3 were carried out, showing the dependence of the magnetic moment on Cu-O-Cu angles.

1. Introduction

Ligands bearing N-heterocyclic groups have become a staple of the coordination chemists' research [1–4]. Pyridines are perhaps the most well-known representatives of this family [5,6], but another family, azoles, has been increasingly gaining prominence over the last decades [7–9], as their charged nature allows the formation of stronger coordination bonds when compared to pyridines. Moreover, functionalized azoles acting as multi-topic ligands are the focus of current interest. The incorporation of those different functional groups greatly increases the available coordination modes and conformations of the ligands, as well as the presence of interesting phenomena such as hemilability or selective coordination to different metal centres [7,9]. They also pave the way for the tailoring of its supramolecular network, allowing the incorporation of supramolecular synthons to the azole backbone.

Of particular interest are those azoles that contain a potentially coordinating dinitrogen moiety (N–N), like pyrazoles [10,11]. In fact, they are known to adopt a variety of coordination modes [11], acting as NN'-bridging ligands and forming distinctive cyclic complexes when deprotonated. On the contrary, when protonated, they act as N-monodentate ligands. They also possess the interesting ability to be easily functionalized in 1-(N-substitution), 3-, 4- and 5- positions, in a variety of manners, such as before the formation of the ring, N-alkylation, or by direct reaction over different functional groups [12–15]. Thus, the pyrazole units act as a framework upon which different functional groups can be incorporated.

Our group has a long trajectory in the design, synthesis, and characterization of pyrazole derived ligands. In the past two decades our efforts have been focused in 1-, 3- and 5- trisubstituted ligands, and, particularly, in incorporating new functional groups in position 1-. For instance, pyrazole ligands bearing groups such as amines [16,17], thioethers [18], sulfoxides/sulfones [19], phosphines [20], phosphinites [21] and alcohols [22] have been obtained, and their coordination behaviour against different metal salts studied. In this sense, we have recently reported the coordination behaviour of one N,O-hybrid pyrazole ligand (2-(3,5-dimethyl-1H-pyrazol-1-yl) ethanol against different Cu(II) salts [23]. The morphology of the resulting complexes shows a direct dependence on the protonation of the alcohol moiety, which results in the formation of dimers or polymers when deprotonated or in the formation of monomers or ionic complexes when protonated.

Following this previous work, we decided to study the behaviour of another two N,O-hybrid ligands with two different aromatic substituents in positions 3,5-: phenyl (2-(3,5-diphenyl-1H-pyrazol-1-yl)ethanol, HL1) or pyridine (2-(3,5-di(2-pyridyl)-1H-pyrazol-1-yl)ethanol, HL2) against CuCl2·2H2O and Cu(NO3)2·3H2O. In recent reports, it has been seen that the inclusion of ligands appended with hydrogen or π donor groups could promote second coordination sphere interactions leading to significant changes in the supramolecular structure and host–guest recognition interactions of the resulting coordination complexes [24–26]. Thus, by incorporating aromatic substituents in the pyrazole framework, the second coordination sphere interactions may promote molecular and supramolecular architectures differing significantly of those obtained with 2-(3,5-dimethyl-1H-pyrazol-1-yl)ethanol [23]. Moreover, recent reports stress the importance of similar ligands in the field of catalysis, as the use of dipyridyl substituents linked by fivemembered ring spacers (such as pyrazole), greatly increase the catalytic ability of those substituents to interact with incoming substrates [27].

On this basis, in this work four coordination complexes bearing the aromatically substituted pyrazole ligands HL1 and HL2 have been isolated: [CuCl(μ-L1)]2·HL1 (1), [CuCl2(HL2)]·H2O (2A), [Cu(NO3)(3,5-hdppz)(μ-L1)]2·2CH3CN (3), (3,5-hdppz = 3,5-diphenylpyrazole) and [Cu(H2O)(3,5-dpypz)]2(NO3)2·H2O (4), (3,5-dpypz = 3,5-(2-pyridyl) pyrazolate) (Scheme 1), which were fully characterized, and their crystal structures elucidated. For complexes 3 and 4 a spontaneous cleavage of the ligands along the NPz-C was observed, resulting in the presence of the corresponding N-unsubstituted pyrazole ligand in their structures. Moreover, it was also observed that upon recrystallization of 2A in CH2Cl2, the resulting complex contained uncoordinated CH2Cl2 molecules, [CuCl2(HL2)]·H2O·CH2Cl2 (2B). The discussion of the molecular and supramolecular structures is presented. Finally, the magnetic properties and magneto-structural correlations for 3 were also determined.

2. Results and discussion

2.1. Synthesis and general characterization

All reactions in this work were carried out using the same solvent, as the drastic effects of the reaction solvent in the molecular structure of coordination complexes bearing similar pyrazole derived ligands is well documented [28,29]. Reaction of HL1 or HL2 against CuCl2·2H2O was carried out via dropwise addition of the metal salt to the corresponding ligand in a 1:1 metal to ligand ratio, in methanol solutions. The reaction mixtures were stirred at r.t. for 48 h. After that period, if no precipitate had appeared, the solutions were concentrated and left overnight in the fridge until its obtaining. Suitable crystals of the resulting complexes were obtained by recrystallization in MeOH or CH2Cl2, respectively. Their single crystal X-ray structure revealed that complex 1 had an uncoordinated HL1 ligand molecule in its structure, thus resulting in [CuCl (μ-L1)]2·HL1 (1). For 2A, it was observed that upon recrystallization in CH2Cl2, some of these solvent molecules were present in its crystal structure, yielding [CuCl2(HL2)]·H2O·CH2Cl2 (2B) (Scheme 1).

The reactivity of HL1 and HL2 against Cu(NO3)2·3H2O was also assayed, using the same procedure as the one described for the synthesis of 1 and 2A. Single crystals suitable for X-ray diffraction were obtained by recrystallization in CH3CN or CH3CN:CHCl3 mixture (3:1 ratio), respectively. Their structure revealed them as [Cu(NO3)(3,5-hdppz) (μ-L1)]2·2CH3CN (3), (3,5-hdppz = 3,5-diphenylpyrazole) and [Cu (H2O)(3,5-dpypz)]2(NO3)2·H2O (4), (3,5-dpypz = 3,5-(2-pyridyl)pyrazolate) (Scheme 1).

Our group had previously reported a NPz-C ligand cleavage for 1-hydroxymethylpyrazole ligand [30], but this is the first time that we report this behaviour for 2-hydroxyethylpyrazole ligand. In a report, Baruah et al. [31], observed a NPz-C cleavage for N-benzoyl-3,5-dimethylpyrazole upon reaction with Cu(NO3)2·3H2O.

Based on these precedents, the presence of the 3,5-hdppz or 3,5-dpypz ligands in the structures may be caused by a similar cleavage of HL1 and HL2. This hypothesis also ties in nicely with the simultaneous presence of HL1 and 3,5-hdppz in complex 3, which to the best of our knowledge, is one of the scarce examples of a complex having simultaneously two different pyrazole ligands coordinated to its metal centre. On the other hand, for 4, all ligand HL2 is cleaved, resulting in the presence of only 3,5-dpypz. This behaviour is in stark contrast with the results obtained for CuCl2·2H2O, where the ligands remained intact,

suggesting that the NPz-C cleavage can be due to the reaction of the ligands with Cu(NO3)·3H2O, much like in the case of Baruah et al [31].

Moreover, when considering our previously published results of the reactivity of the similar 3,5-disusbstituted ligand 2-(3,5-dimethyl-1Hpyrazol-1-yl)ethanol against Cu(NO3)2·3H2O [23], where the ligand remained intact, this behaviour is even more striking. This suggests that electronic effects caused by the substituents in positions 3- and 5- to the pyrazole ring may result in the NPz-C bond being more susceptible to cleavage promoted by the Cu(NO3)2·3H2O. In this sense, the 13C{1H} NMR spectra of 2-(3,5-dimethyl-1H-pyrazol-1-yl)ethanol, HL1 and HL2 show a progressive downfield shift of the C-NPz: 49.8 ppm [32], 51.3 ppm [33] and 52.7 ppm [34], respectively, suggesting that the carbon atoms in HL1 and HL2 are more deshielded than those of 2-(3,5-dimethyl-1H-pyrazol-1-yl)ethanol.

All complexes were characterized by analytical and spectroscopic techniques. Spectroscopic details of their characterization can be found in the Exp. Sect. and Supporting Information (S.I.). Elemental analyses (EA) of all complexes agreed with the proposed formulae, except for 2B, as the solvent molecules of CH2Cl2 were readily lost during sample preparation for EA.

Conductivity values were registered in MeOH (1, 2A) or CH3CN (3, 4) in concentrations around 1·10-3 M. The measured conductivity values for 1 – 3 were small, ranging from 14 to 57 Ω-1cm2mol-1, agreeing with the presence of non-electrolytes [35]. For complex 4, on the other hand, the measured value was 219 Ω-1cm2mol-1 agreeing with the presence of a 2:1 electrolyte complex [35].

The FTIR-ATR spectra of the four complexes in the range of 4000–500 cm-1 confirmed the coordination of the ligand to the metal center (S.I. Fig. S1-S4). The most characteristic bands of the IR spectra were those corresponding to [ν(C–C/C–N)ar] (1614–1551 cm-1), [δ(C–C/C–N)ar] (1464–1438 cm-1), [δ(C–H)ip] (1073–1016 cm-1) and [δ(C–H)oop] (781–688 cm-1) [36]. These signals were attributable to the pyrazole and phenyl rings present in the ligands. For complex 1, since both deprotonated coordinated and protonated uncoordinated HL1 were present in the molecule, the signals were broad, as the signals of both ligands overlapped. The region between 3600 and 3100 cm-1 was also relevant for the characterization of these complexes, since it hosted signals attributed to [ν(O–H)]. Thus, for complexes 1, 2A and 4 broad bands centred at 3532–3121 cm-1 were

identified, attributed to the alcohol moieties of HL ligands or water molecules. For complex 2A, this region was especially remarkable, as two distinct [ν(O–H)] [37] signals were identified, one corresponding to coordinated HL2 at 3532 cm-1 and one corresponding to solvent water molecules at 3246 cm-1. Moreover, for complex 3, a small band was observed at 3122 cm-1 but owing to its shape and neighbouring flat region was attributed to [ν(N–H)] [37]. In this same complex, a small band appeared at 2254 cm-1 which was attributed to [ν(CN)] of the occluded acetonitrile molecules. Finally, for complexes 3 and 4, signals attributed to [ν(NO3)] [37] appeared at 1453–1389 cm-1 and 1300–1268 cm-1. Regarding those same groups, between 1800 and 1700 cm-1, signals attributed to ν1 + ν4 vibrations were observed [38]. For complex 3, two signals at 1750 and 1741 cm-1 were identified, which agreed with a monodentate coordination mode, whereas for 4, only one band at 1749 cm-1 was observed, indicative of the presence of ionic nitrates [38].

The UV–Vis spectra have been recorded in MeOH for 1 and 2A (≈ 1·10-3 M), and in CH3CN for 3 and 4 (≈ 1·10-3 M) (Figs. S5 and S6). All the spectra showed one band in the visible region between 709 and 769 nm. The ε values were between 66 and 154 M-1cm-1. These bands are typical of Cu(II) metal centers in a square planar or square pyramidal coordination and were assigned to a 2B1g to 2A1g transitions [39–41]. All ε values were consistent with Laporte-forbidden transitions [40].

2.2. Crystal and extended structure of 1

Complex 1 crystallizes in the monoclinic crystal system having a C2/ c space group. It has a dimeric structure with a Cu:L1:Cl 1:1:1 ratio and possesses an HL1 molecule in its second coordination sphere (Fig. 1). Contrary to most of the reported dimers with other N-hydrox- yethylpyrazoles [22,23,42–45], 1 is an asymmetric dimer, displaying two different distorted square planar Cu(II) atom cores. The first one, [CuO2Cl2] (τ4 = 0.22) [46], contains two terminal chlorine atoms, with Cu-Cl bond lengths ranging from 2.2230(8) Å to 2.2397(7) Å (Table 1), and two bridging oxygens provided by the pyrazole ligand, Cu–O bond lengths being shorter, ranging from 1.9391(17) Å to 1.9686(17) Å (Table 1). The second one, [CuO2N2] (τ4 = 0.26) [46], is coordinated exclusively to the pyrazole ligand, sharing the bidentate oxygens of the first core (Cu–O bond lengths at 1.8958(16) and 1.9062(17) Å, Table 1) and completing their coordination with the nitrogen atoms (Cu–N bond lengths at 1.945(2) and 1.961(1) Å, Table 1). The coordinated pyrazole ligands are deprotonated, acting as bidentate bridging and chelate li- gands, having a NPz-Cu-Oal of

91.23(9)◦. The steric constraints induced by the presence of the bulky substituents in positions 3,5-, coupled with the chelate behaviour of the ligands, may be the cause of the distortion of the square planar cores, with angles ranging from 76.09(7)◦ to 94.77 (5)◦ and 156.68(9)◦ to 168.11(5)◦ (Table 1). Selected bond distances and angles for 1 are summarized on Table 1. They are in agreement with reported Cu(II) pyrazole complexes [32,33]. Our research group has previously reported the synthesis of [CuCl(μ-L1)]2·CH3NO2 [33], which possesses a nitromethane solvent molecule. In both cases, the solvent molecules in the second coordination sphere play key roles in their respective supramolecular architectures.

The disorder in the HL1 ligand present in the second coordination sphere prevents an in-depth study of complex's 1 supramolecular scaffold. Despite this hindrance, it can be observed that pairs of dimeric units are associated via H···Cl interactions, involving hydrogen groups of the phenyl ring of coordinate L1. Then, those pairs of dimers units are linked together thanks to interactions involving the oxygen atoms of uncoordinated HL1 and hydrogen atoms of the phenyl rings from co- ordinated L1. Overall, the pairs of dimers and the occluded solvents are disposed in alternate layers. The non-coordinated ligand molecules occupy isolated cavities accounting for a remarkable 20.2% of its unit cell volume (1543.68 Å3) (Fig. 1). The values of intermolecular interactions are summarized in Table 1.

2.3. Crystal and extended structure of 2B

Complex 2B crystallizes in the triclinic crystal system having a P-1 space group. It has a monomeric structure having a Cu:HL2:Cl 1:1:2 ratio (Fig. 2). Moreover, it contains both H2O and CH2Cl2 as occluded solvents. Its [CuON2Cl2] core has a slightly distorted square pyramidal geometry (τ5 = 0.22) [47]. This slight distortion is reflected in the bond angles, which range between 79.50(3)◦ to 105.162(11)◦ and from 153.75(3)◦ to 166.79(3)◦ (Table 2). The basal plane is formed by two nitrogen atoms and one oxygen atom from the HL2 ligand (Cu–O bond length at 1.9985(8) Å, and Cu–N ranging from 1.9805(8) Å to 2.0261(9) Å, Table 2), and a chlorine atom lying at a longer distance (Cu-Cl bond length being 2.2322(3) Å, Table 2), while the apical position is occupied by the last chlorine atom (Cu-Cl bond length at 2.4818(4) Å, Table 2). Thus, HL2 acts as a tridentate chelate ligand, coordinating via its Npyrazol, N-pyridine and HO-alcohol moieties. The NPz-Cu-NPy and NPz-Cu-Oal bite angles are 79.50(3)◦ and 87.45(3)◦, respectively. Selected bond distances and angles are reported in Table 2. They are in agreement with similar Cu(II) nitrate pyrazole complexes [48,49].

The presence of H2O and CH2Cl2 dictates the supramolecular architecture in 2B. Thus, sets of two H2O molecules link four monomers forming a double linear chain along a axis. The chlorine atoms and the hydrogen of alcohol moieties are heavily involved in this scaffold (Fig. 2, Table 2). Nestled among those chains, lie the CH2Cl2 molecules, forming a clathrate-like structure (Fig. 2). Overall, these CH2Cl2 molecules occupy isolated cavities representing 13.0% of its unit cell volume (128.87 Å3, measured with a prove radius of 1.2 Å). Taking H2O molecules into consideration, the cavities nestling the solvents account for 15.9% of its unit cell volume (157.39 Å3, measured with a prove radius of 1.2 Å, Fig. S7).

2.4. Crystal and extended structure of 3

Complex 3 crystallizes in the triclinic crystal system having a P-1 space group. It has a dimeric structure having a Cu:L1:3,5-hdppz:NO3 1:1:1:1 ratio (Fig. 3). Moreover, it contains CH3CN molecules. Its [CuO3N2] core displays a slightly distorted square pyramidal geometry ($\tau5 = 0.14$) [47]. The apical position is occupied by the oxygen atom of the nitrate group, displaying a Cu–O bond length of 2.474(1) Å (Table 3), while the rest of the atoms, namely two oxygens and one nitrogen provided by L1 and one nitrogen provided by 3,5-hdppz, are in the basal plane, Cu–O bond lengths ranging from 1.9008(10) Å to 1.9501(10) Å and Cu–N from 1.9505(11) Å to 2.0251(11) Å (Table 3). The L1 ligands acts as a chelated and bridged ligand, NPz-Cu-Oal bite angle being 93.27(4)◦, while the nitrate moiety coordinates in a monodentate fashion. Selected bond lengths and angles are summarized in Table 3. As stated before, the presence of the 3,5-hdppz ligand in this complex owes to the cleavage of the HL1 ligand. The 3,5-hdppz ligand remains protonated, thus acting as a neutral monodentate ligand.

The supramolecular scaffold of 3 is dominated by the interaction between uncoordinated oxygens of the nitrate group and the hydrogen of the pyrazole ligand. This results in the formation of supramolecular 1D-chains parallel to the a axis. Moreover, the solvent molecules in the second coordination sphere also play a role in holding the supramolecular structure, binding together these supramolecular chains in 2D planes. Finally, it is remarkable that the presence of multiple phenyl groups in positions 3- and 5- result in the formation of C–H···π interactions, which bind the planes completing the 3D structure (Fig. 4).

The second coordination sphere's solvents occupy isolated cavities, accounting for 6.3% (96.15 Å3) of its unit cell volume (Fig. S7). The values of intermolecular interactions are summarized in Table 3.

2.5. Crystal and extended structure of complex 4

Complex 4 crystallizes in the orthorhombic crystal system having a Fddd space group. During the synthesis of complex 4, ligand HL2 is cleaved, yielding an ionic complex bearing a dimeric cation and two nitrate anions. Moreover, three water molecules are also present in its crystal structure, as each of the two Cu(II) metal centres is coordinated to one and a further water molecule is present in the second coordination sphere. Thus, the cation possesses a Cu:3,5-dpypz:H2O 1:1:1 ratio (Fig. 5).

The Cu(II) atoms display an almost perfect square pyramidal geometry (τ5 = 3.3·10-3) [47] with a [CuN4O] core. The nitrogen atoms of the 3,5-dpypz ligands form the basal plane. Note that azo nitrogen atoms bond lengths are shorter (1.960(5) Å, Table 4) than those of the pyridine nitrogen atoms (ranging from 2.077(5) to 2.097(5) Å, Table 4) and the oxygen atom of the water molecules are in the apical positions (Cu–O bond length being 2.207(4) Å, Table 4). It is also worth noting that the ligand is deprotonated, thus acting as a tetracoordinate pyrazolate ligand. The pyrazolate ligands with hydrogens in positions 3- and 5- are known to coordinate by both of their nitrogen groups, forming trimeric or polymeric structures [8,50]. However, the addition of bulky substituents on these positions prevents the formation of these motifs due to steric constraints, resulting in the formation of dimers, as reported in different publications by our group [51–55] and other authors [56–59]. Moreover, the presence of the pyridine substituent may promote a chelate behaviour of the ligand [60–64]. Thus, based on these precedents, the chelating and bridging behaviour of the 3,5-dpypz ligand is clearly rationalized. In fact, the dihydrate analogue of 4, ([Cu(H2O)(3,5-dpypz)]2(NO3)2·2H2O), has already been synthesized in our group [65]. This chelate behaviour is reflected in the Npyr-Cu-NPz angles of the same ligand (ranging from 79.70(18) to 79.81(18)◦, Table 4), which are smaller than the ideal 90◦ for a square pyramidal coordination geometry, but is compensated by the bigger Npyr-Cu-NPyr angles of different ligands (ranging from 104.99(19)◦ □ 107.63(19)◦, Table 4) accounting for its small τ5 value. Meanwhile, all N-Cu–O angles to the apical oxygen range from 85.93(19)◦ to 96.43(17)◦ (Table 4). Relevant bond lengths and angles for complex 4 are summarized in Table 4. They agree with similar complexes reported in the literature [57–59,65].

Owing to the presence of some disorder in nitrate anions and second coordination sphere's water molecules in complex 4, its supramolecular scaffold cannot be studied precisely. However, it is clearly dominated by the formation of strong O–H···O hydrogen bonds between both types of water molecules (coordinated and uncoordinated) and nitrate anions. Thus, the overall supramolecular packing could be described as alternating layers of nitrate anions and dimeric cations, with the occluded water molecules embedded in the cationic layer (Fig. 5b). Moreover, π-π stacking interactions between pyridyl rings of the cations are identified, as pyridyl rings lie completely parallel to each other at 3.487 Å and 3.862 Å (Fig. 5c). In this arrangement, water molecules occupy isolated cavities which account for 1.0% of its unit cell volume (113.34 Å3, measured with a prove radius of 1.2 Å, Fig. S7). The intermolecular interactions are summarized in Table 4.

2.6. Magnetic susceptibility measurements of 3

Solid-state, variable temperature (5–300 K) magnetic susceptibility data was collected for 3 using a 100 Oe field (Fig. 6). Its XpT value at 300 K is 0.325 cm3mol-1, lower than the expected for two uncoupled S = ½ assuming g = 2.00 (0.75 cm3mol-1). Upon decreasing temperature, this value decreases almost linearly to a value of 0.232 cm3mol-1, at 5 K, suggesting a strong antiferromagnetic interaction. The experimental data were fitted using the Bleany-Bowers equation [66] for binuclear copper(II) complexes with the Hamiltonian in the form H = -JS1S2. The best fit parameters in the temperature range from 5 to 300 K were found for: g = 2.10, ρ = 2.94% and 2J = -539 cm-1. These values are similar to those reported for complex [CuCl(μ-L1)]2·CH3NO2 (g = 2.16, and 2J = -572 cm-1) [33], and similar alkoxide bridged dimers [23] and agree to Haase's magneto-structural correlations [67]. However, it is important to note that for strong antiferromagnetic complexes, where the diamagnetic correction is of the same order of magnitude as the un- corrected molar susceptibility, uncertainty of the corrected values is large, thus uncertainty of the estimated 2J values is 5–10% [68–70]. Despite this, trends can still be assessed.

Previous studies show that the magnetic interaction value in alkoxo- bridged Cu(II) dimers strongly depends on their topological features. The consensus is that six of them are key: (i) Cu···Cu distance, (ii) Cu–O- Cu angle (θ), (iii) Cu–O distance, (iv) torsional angle (angle of the carbon bonded to the bridging oxygen atom, τ), (v) planarity of the bonds around the bridging oxygen and (vi) hinge distortion (roof shape) [67,71–74]. However, it has been stablished that parameters (i), (ii), and (iii) show some intrinsic relationship [72–

74], thus Cu–O-Cu angle is the main parameter for predicting 2 J values. For complex 3, the sum of the angles around the bridging oxygen is 374.35◦, has a θ value of 104.30◦, a τ value of 16.3◦, and no hinge distortion is observed. Owing to these parameters, the antiferromagnetic interactions agree with the reported models.

3. Conclusions

We have tested the reactivity of two hybrid N,O- donor pyrazole derived ligands, (HL1 and HL2) against different Cu(II) salts: $CuCl_2 \cdot 2H_2O$ and $Cu(NO_3)_2 \cdot 3H_2O$, yielding complexes 1–4. All complexes were fully characterized. The crystal structure of all the resulting complexes was elucidated, showing diverse topologies such as asymmetrical dimers (1), monomers (2B), symmetrical dimers (3) and ionic (4). Moreover, it showed that those ligands are cleaved along the NPz-C bond upon reaction with $Cu(NO_3)_2 \cdot 3H_2O$, resulting in the in situ formation of two disubstituted pyrazole ligands: 3,5-diphenylpyrazole and 3,5-di(2-pyridyl)pyrazolate. As a result, a complex bearing two different pyrazole ligands in its structure has been isolated (3). Lastly, the magneto structural correlations in 3 were studied. This complex shows strong antiferromagnetic behaviour, which can be rationalised based on their Cu–O-Cu angle and τ values.

4. Experimental Section

4.1. Materials and general details

Copper(II) chloride dihydrate (CuCl2·2H2O), copper(II) nitrate tri- hydrate (Cu(NO3)2·3H2O), 2-hydroxyethylhidrazine, 1,3-diphenyl-1,3- propanedione, 1,3-di(2-pyridyl)-1,3-propanedione, methanol (MeOH), ethanol (EtOH), diethyl ether (Et2O), acetonitrile (CH3CN), dichloro- methane (CH2Cl2) and chloroform (CHCl3) were purchased from Sigma Aldrich and used without further purification. Reactions and manipulation were carried out in air at room temperature (r.t.). The 2-(3,5- diphenyl-1H-pyrazol-1-yl) ethanol (HL1) and 2-(3,5-(2-dipyridyl)-1H- pyrazol-1-yl)ethanol (HL2) were synthesised as described in the literature [27,28]. Elemental analyses (EA) (C, H, N) were carried out on a Thermo Scientific Flash 2000 CHNS Analyses. Conductivity measurements were performed at r.t. in MeOH (1, 2A) or CH3CN (3, 4) solutions ($\approx$ 1·10-3 M), using an EC-Meter BASIC 30 (Crison Instruments) conductometer. FTIR-ATR spectra were recorded on a Tensor 27 (Bruker) spectrometer, equipped with an attenuated total reflectance (ATR) accessory model MKII Golden Gate with diamond window in the range 4000–600 cm-1. The electronic spectra in MeOH (1, 2A) or CH3CN (3, 4) solutions (5.96·10-4-1.32·10-3 M) were run on a JASCO V-780 UV–Visible/NIR Spectrophotometer with a quartz cell having a path length of 1 cm in the range of 500–1100 nm. Magnetic measurements from 5 K to 300 K were carried out with a Quantum Design MPMS-5S SQUID spectrometer using a 100 Oe field. The experimental susceptibilities were corrected for the diamagnetism of the constituent atoms [75] and effects of the capsule container.

4.2. Synthesis of complex [CuCl(μ-L1)]2·HL1 (1)

To a solution of HL1 (1.01 mmol, 0.266 g) in MeOH (15 mL), a solution of CuCl2·2H2O (1.00 mmol, 0.171 g) in MeOH (10 mL) was added dropwise. The resulting dark green solution was stirred for 48 h at r.t. After that period, the solution was concentrated up to 5 mL and left overnight on the fridge, resulting in the formation of a dark green solid. This solid was filtered off, washed with cold Et2O (5 mL) and dried under

vacuum. Suitable crystals for X-ray diffraction of complex 1 were ob- tained by recrystallization in MeOH for six days.

1. Yield: 27.9% (0.090 g). Elem. Anal. Calc. for C85H76Cl4Cu4N2O5 (1713.56 g/mol): C 59.32; H 4.19; N 8.12. Found: C 59.22; H 4.08; N 7.95%. Conductivity (1.06·10-3 M in MeOH): 57 Ω-1·cm2·mol-1. FTIR- ATR (wavenumber, cm-1): 3331(br) [ν(O–H)], 3056(w) [ν(C–H)ar], 2941–2851(w) [ν(C–H)al], 1576(m) and 1551(m) [ν(C–C/C–N)]ar, 1469(m), 1464(m) and 1451(m) [δ(C–C/C–N)]ar, 1374(m), 1298(m), 1278(m), 1235(w), 1202(w), 1160 (w), 1102(w), 1073(m) and 1016(m) [δ(C–H)ip], 965(w), 922(w), 879(w), 809(w), 761(vs) [δ(C–H)oop] and 695(vs) [δ(C–H)oop], 614(w), 580(w), 519(w). UV–Vis: (MeOH, 8·92·10-4 M) ʎmax (ε(M-1cm-1)) = 769 nm (66).

4.3. Synthesis of complex [CuCl2(HL2)]·H2O (2A)

To a solution of HL2 (0.635 mmol, 0.169 g) in MeOH (10 mL), a solution of CuCl2·2H2O (0.635 mmol, 0.285 g) in MeOH (20 mL) was added dropwise. The resulting dark green solution was stirred for 48 h at r.t. After that period, a green precipitate appeared, which was filtered off, washed with cold Et2O (5 mL) and dried under vacuum. Suitable crystals for X-ray diffraction of the complex were obtained by recrystallization in CH2Cl2 for two weeks. The single X-ray crystal analysis revealed the presence of CH2Cl2 in its structure, thus resulting in com- plex [CuCl2(HL2)]·H2O·CH2Cl2 (2B). However, for samples of 2B, the molecules of CH2Cl2 are readily lost in contact with the atmosphere, even for single crystals, preventing its spectroscopical and analytical characterization. Thus, EA results were adjusted considering [CuCl2(HL2)]·H2O (2A). 2A. Yield: 72.2% (0.231 g). Elem. Anal. Calc. for C14H16Cl2CuN4O2 (406.75 g/mol): C 41.34; H 3.96; N 13.77. Found: C 41.27; H 4.08; N 13.49%. Conductivity (1.3·10-3 M in MeOH): 14 Ω-1·cm2·mol-1. FTIR- ATR (wavenumber, cm-1): 3532(br) and 3246(br) [ν(O–H)], 3113 (m)-3032(m) [ν(C–H)ar], 2969(w)-2932(w) [ν(C–H)al], 1609(m) [ν(C–C/C–N)]ar, 1586(m) and 1567(m) [ν(C–C/C–N)]ar, 1466(w), 1442(m) and 1438(s) [δ(C–C/C–N)]ar, 1380(m), 1351(m), 1314(w), 1286(m), 1252(w), 1229(w), 1161 (m), 1043(s) [δ(C–H)ip], 1013(m), 978(m), 880(w), 848(m), 826(m), 795(m), 781(s) [δ(C–H)oop], 741(w), 738(m), 685(m), 659(w), 626(m). UV–Vis: (MeOH, 1.32·10-3 M) ʎmax (ε(M-1cm-1)) = 769 nm (68).

4.4. Synthesis of [Cu(NO3)(3,5-hdppz)(μ-L1)]2·2CH3CN (3), (3,5- hdppz = 3,5-diphenylpyrazole)

To a solution of HL1 (1.69 mmol, 0.474 g) in MeOH (20 mL), a solution of Cu(NO3)2·3H2O (1.79 mmol, 0.432 g) in MeOH (20 mL) was added dropwise. The resulting dark green solution was stirred for 48 h at r.t. After that period, the solution was

concentrated up to 5 mL, and left standing to evaporate for four days. Then, the green precipitate was filtered off, washed with cold Et2O (5 mL) and dried under vacuum. Recrystallization of this solid in CH3CN for two weeks yielded suitable crystals for X-ray diffraction.

3. Yield: 89.55% (0.492 g). Elem. anal. Calc. for C68H60Cu2N12O8 (1300.36 g/mol): C 62.81; H 4.65; N 12.93. Found: C 62.59; H 4.36; N 12.78%. Conductivity (5.69·10-4 M in CH3CN): 44 Ω-1·cm2·mol-1. FTIR-ATR (wavenumber, cm-1): 3122(w) [ν(N–H)], 3061(w) [ν(C–H)ar], 2915(w)-2863(w) [ν(C–H)al], 2254(m) [ν(CN)], 1750–1741(w) [ν1 + ν4 (NO3)], 1577(s)-1551(s) [ν(C–C/C–N)]ar, 1478(m), 1464(m) [δ(C–C/C–N)]ar, 1441(m), 1389(vs) [ν(NO3)], 1300(vs) [ν(NO3], 1233(w), 1204(w), 1161(m), 1104(m), 1076(s) [δ(C–H)ip], 1038(m), 1028(m), 1016(m), 990(m), 986(m), 968(w), 954 (w), 910(m), 843(w), 811(w), 758(vs) [δ(C–H)oop], 705(w), 689(vs) [δ(C–H)oop], 669 (m), 648(w), 579(m). UV–Vis: (CH3CN, 5.69·10-4 M) ʎmax (ε(M-1cm-1)) = 728 (154).

4.5. Synthesis of [Cu(H2O)(3,5-dpypz)]2(NO3)2·H2O (4), (3,5-dpypz = 3,5-di(2-pyridyl)pyrazolate)

To a solution of HL2 (0.37 mmol, 0.098 g) in MeOH (20 mL), a solution of Cu(NO3)2·3H2O (0.39 mmol, 0.094 g) in MeOH (20 mL) was added dropwise. The resulting dark green solution was stirred for 48 h at r.t. After that period, the solution was concentrated up to 5 mL, and left in the fridge for two days, resulting in the formation of a green precipitate. Then, the green precipitate was filtered off, washed with cold Et2O (5 mL) and dried under vacuum. Recrystallization of this solid in a CH3CN:CHCl3 mixture (3:1) for one month yielded suitable crystals for X-ray diffraction.

4. Yield: 71.24% (0.098 g). Elem. anal. Calc. for C26H24Cu2N10O9 (747.63 g/mol): C 41.77; H 3.24; N 18.74. Found: C 41.62; H 3.30; N 18.53%. Conductivity (6.95·10-4 M in CH3CN): 219 Ω-1·cm2·mol-1. FTIR-ATR (wavenumber, cm-1): 3301(br) [ν(OH)], 3099(w)-2952(w) [ν(C–H)ar + ν(C–H)al], 1749(w) [ν1 + ν4 (NO3)], 1614(s) [ν(C=/=N)]ar, 1588(s) and 1569(s) [ν(C–C/C–N)]ar, 1472(m), 1461(m) [δ(C–C/C–N)]ar, 1435(s) [ν(NO3)], 1406(m), 1361(m), 1271(vs) [ν(NO3], 1158(m), 1053(w), 1046(m), 1036(s) [δ(C–H)ip], 1017(m), 993(m),980(w), 955(m), 891(w), 870(m), 840(w), 820(m), 799(m), 781 (vs) [δ(C–H)oop], 750(s) [δ(C–H)oop], 716(m), 984(m), 656(m), 648 (m), 626(m), 596(m). UV–Vis: (CH3CN, 6.95·10-4 M) ʎmax (ε(M-1cm-1)) = 709 nm (119).

4.6. X-ray crystallography

Blue (1, 3 and 4) or green (2B) prism-like specimens were used for the X-ray crystallographic analysis. The X-ray intensity data were measured on a D8 Venture system equipped with a multilayer monochromator and a Mo microfocus (λ = 0.71073 Å). The frames were integrated with the Bruker SAINT software package using a narrow-frame algorithm. For 1, the integration of the data using a monoclinic unit cell yielded a total of 67927 reflections to a maximum θ angle of 26.54◦ (0.80 Å resolution), of which 7851 were independent (average redundancy 8.652, completeness = 98.4%, Rint = 8.91%, Rsig = 4.48%) and 5742 (73.14%) were greater than 2σ(F2). For 2B, the integration of the data using a triclinic unit cell yielded a total of 38964 reflections to a maximum θ angle of 30.62◦ (0.70 Å resolution), of which 5964 were independent (average redundancy 6.533, completeness = 97.9%, Rint = 2.53%, Rsig = 1.60%) and 5747 (96.36%) were greater than 2σ(F2). For 3, the integration of the data using a triclinic unit cell yielded a total of 63778 reflections to a maximum θ angle of 30.55◦ (0.70 Å resolution), of which 9331 were independent (average redundancy 6.835, completeness = 99.8%, Rint = 3.55%, Rsig = 2.22%) and 8326 (89.23%) were greater than 2σ(F2). For 4, the integration of the data using an orthorhombic unit cell yielded a total of 70886 reflections to a maximum θ angle of 31.06◦ (0.69 Å resolution), of which 4701 were independent (average redundancy 15.079, completeness = 99.7%, Rint = 10.15%, Rsig = 4.16%) and 2749 (58.48%) were greater than 2σ(F2). The structures were solved and refined using the Bruker SHELXTL Software Package [76].

Crystal data and relevant details of structure refinement are reported in Table 5. Molecular graphics were generated with Mercury 4.1.3 [77,78] with POV-Ray package [79]. Color codes for molecular graphics: grey (C), white (H), green (Cl), red (O), blue (N), orange (Cu).

CRediT authorship contribution statement

Joan Soldevila-Sanmartín: Investigation, Visualization, Writing – original draft. **Teresa Calvet:** Validation, Resources, Funding acquisition, Writing – review & editing. **Mercè Font-Bardia:** Validation, Formal analysis, Data curation. **José G. Planas:** Resources, Supervision, Project administration, Funding acquisition. **Josefina Pons:** Conceptualization, Validation, Resources, Writing – review & editing, Supervision, Project administration, Funding acquisition.

Declaration of Competing Interest

The authors declare that they have no known competing financial interests or personal relationships that could have appeared to influence the work reported in this paper.

Acknowledgements

J.P. thanks CB615921 project, the CB616406 project from “Fundacio´ La Caixa” and the Generalitat de Catalunya (2017/SGR/1687). T.C. thanks the Spanish National Plan of Research MAT2015-65756R. J.G.P. thanks MINECO (PID2019-106832RB-I00), MICINN through the Severo Ochoa Program for Centers of Excellence for the FUNFUTURE (CEX2019-000917-S and MDM-2017-0767 projects) and the Generalitat de Catalunya (2017/SGR/1720 and SGR2017-1289). J.S. also ac- knowledges the PIF pre-doctoral Fellowship from the Universitat Autònoma de Barcelona for his pre-doctoral grant.

References

[1] I. Haiduc, J. Coord. Chem. 72 (2019) 2127–2159, https://doi.org/10.1080/00958972.2019.1641702.

[2] I. Haiduc, J. Coord. Chem. 72 (2019) 2805–2903, https://doi.org/10.1080/00958972.2019.1670349.

[3] R.H. Crabtree (Editor), Coord. Chem. Rev. 251 (2007) 595-896. https://doi.org/ 10.1016/j.ccr.2006.08.005.

[4] A.V. Desai, S. Sharma, S. Let, S.K. Ghosh, Coord. Chem. Rev. 395 (2019) 146–192, https://doi.org/10.1016/j.ccr.2019.05.020.

[5] A.Y. Robin, K.M. Fromm, Coord. Chem. Rev. 250 (2006) 2127–2157, https://doi. org/10.1016/j.ccr.2006.02.013.

[6] P.J. Steel, Acc. Chem. Res. 38 (2005) 243–250, https://doi.org/10.1021/ ar040166v.

[7] G. Aromí, L.A. Barrios, O. Roubeau, P. Gamez, Coord. Chem. Rev. 255 (2011) 485–546, https://doi.org/10.1016/j.ccr.2010.10.038.

[8] J.-P. Zhang, Y. Zhang, J. Lin, X. Chen, Chem. Rev. 112 (2012) 1001–1033, https:// doi.org/10.1021/cr200139g.

[9] S.-Q. Bai, D.J. Young, T.S.A. Hor, Chem. - An Asian J. 6 (2011) 292–304, https:// doi.org/10.1002/asia.201000698.

[10] C. Pettinari, A. T˘aba˘caru, S. Galli, Coord. Chem. Rev. 307 (2016) 1–31, https://doi. org/10.1016/j.ccr.2015.08.005.

[11] M.A. Halcrow, Dalton Trans. (2009) 2059–2073, https://doi.org/10.1039/ b815577a.

[12] I. Alkorta, R.M. Claramunt, E. Díez-Barra, J. Elguero, A. de la Hoz, C. López, Coord. Chem. Rev. 339 (2017) 153–182, https://doi.org/10.1016/j.ccr.2017.03.011.

[13] A. Adach, J. Coord. Chem. 70 (2017) 757–779, https://doi.org/10.1080/00958972.2017.1278572.

[14] S. Fustero, M. Sánchez-Roselló, P. Barrio, A. Simón-Fuentes, Chem. Rev. 111 (2011) 6984–7034, https://doi.org/10.1021/cr2000459.

[15] S. Fustero, A. Simón-Fuentes, J.F. Sanz-Cervera, Org. Prep. Proced. Int. 41 (2009) 253–290, https://doi.org/10.1080/00304940903077832.

[16] G. Aragay, J. Pons, J. Ros, A. Merkoçi, Langmuir 26 (2010) 10165–10170,

https://doi.org/10.1021/la100288s.

[17] A. Pañella, J. Pons, J. García-Antón, X. Solans, M. Font-Bardia, J. Ros, Eur. J. Inorg. Chem. (2006) 1678–1685, https://doi.org/10.1002/ejic.200501056.

[18] J. García-Antón, J. Pons, X. Solans, M. Font-Bardia, J. Ros, Synthesis, Eur. J. Inorg. Chem. (2003) 2992–3000, https://doi.org/10.1002/ejic.200300035.

[19] A. De León, M. Guerrero, J. García-Antón, J. Ros, M. Font-Bardía, J. Pons, CrystEngComm 15 (2013) 1762–1771, https://doi.org/10.1039/c2ce26687c.

[20] M. Guerrero, S. Muñoz, J. Ros, T. Calvet, M. Font-Bardía, J. Pons, J. Organomet. Chem. 799–800 (2015) 257–264, https://doi.org/10.1016/j. jorganchem.2015.10.007.

[21] S. Muñoz, M. Guerrero, J. Ros, T. Parella, M. Font-Bardia, J. Pons, Cryst. Growth Des. 12 (2012) 6234–6242, https://doi.org/10.1021/cg3014333.

[22] M. Guerrero, J. Pons, J. Ros, M. Font-Bardia, O. Vallcorba, J. Rius, V. Branchadell, CrystEngComm 13 (2011) 6457–6470, https://doi.org/10.1039/c1ce05626c.

[23] J. Soldevila-Sanmartín, X. Montaner, T. Calvet, M. Font-Bardia, J. Pons, Polyhedron (2020), 114686, https://doi.org/10.1016/j.poly.2020.114686.

[24] R.L. Shook, A.S. Borovik, Inorg. Chem. 49 (2010) 3646–3660, https://doi.org/10.1021/ic901550k.

[25] S.A. Cook, A.S. Borovik, Acc. Chem. Res. 48 (2015) 2407–2414, https://doi.org/10.1021/acs.accounts.5b00212.

[26] Z.Z. Qu, T.B. Gao, J. Wen, K. Rui, H. Ma, D.K. Cao, Dalton Trans. (2018) 9779–9786, https://doi.org/10.1039/C8DT01922C.

[27] J. Sampson, G. Choi, M.N. Akhtar, E.A. Jaseer, R. Theravaloppil, T. Agapie, ACS Omega 4 (2019) 15879–15892, https://doi.org/10.1021/acsomega.9b01788.

[28] W.L. Driessen, S. Gorter, W.G. Haanstra, L.J.J. Laarhoven, J. Reedijk, K. Goubitz, F. R. Selj´ee, Recl. Trav. Chem. Pays-Bas 112 (1993) 309–313, https://doi.org/10.1002/recl.19931120506.

[29] M. Guerrero, J. Pons, V. Branchadell, T. Parella, X. Solans, M. Font-Bardia, J. Ros, Inorg. Chem. 47 (2008) 11084–11094, https://doi.org/10.1021/ic8013915.

[30] A. Boixassa, J. Pons, X. Solans, M. Font-Bardia, J. Ros, Inorg. Chim. Acta. 355 (2003) 254–263, https://doi.org/10.1016/S0020-1693(03)00346-3.

[31] K. Deka, M. Laskar, J.B. Baruah, Polyhedron 25 (2006) 2525–2529, https://doi.org/10.1016/j.poly.2006.02.019.

[32] W.L. Driessen, B. Maase, J. Reedijk, H. Kooijman, M.T. Lakin, A.L. Spek, Inorg. Chim. Acta 300–302 (2000) 1099–1103.

[33] S. Muñoz, J. Pons, J. Ros, M. Font-Bardia, C.A. Kilner, M.A. Halcrow, Inorg. Chim. Acta 373 (2011) 211–218, https://doi.org/10.1016/j.ica.2011.04.027.

[34] M. Guerrero, T. Calvet, M. Font-Bardia, J. Pons, Polyhedron 119 (2016) 555–562, https://doi.org/10.1016/j.poly.2016.09.004.

[35] W.J. Geary, Coord. Chem. Rev. 7 (1971) 81–122, https://doi.org/10.1016/S0010-8545(00)80009-0.

[36] G. Gliemann, K. Nakamoto: Infrared and Raman Spectra of Inorganic and Coordination Compounds. John Wiley and Sons, New York, Chichester, Brisbane, Toronto, 1978. https://doi.org/10.1002/bbpc.19780821138.

[37] K. Nakamoto in P. Griffiths, J.M. Chalmers (Eds.), Handbook of Vibrational Spectroscopy. John Wiley and Sons, New York, 2006, pp. 1872-1892. https://doi.org/10.1002/9780470027325.s4104.

[38] A.B.P. Lever, E. Mantovani, B.S. Ramaswamy, Can. J. Chem. 49 (1971) 1957–1963, https://doi.org/10.1139/v71-315.

[39] S. Kumar, R. Pal Sharma, P. Venugopalan, V. Singh Gondil, S. Chhibber, T. Aree, M. Witwicki, V. Ferretti, Inorg. Chim. Acta 469 (2018) 288–297, https://doi.org/10.1016/j.ica.2017.09.032.

[40] D. Sutton, Electronic Spectra of Transition Metal Complexes, First, McGraw Hill Publishing Company Ltd., Maidenhead, Berkshire, England, 1975.

[41] F. Sánchez-Férez, M. Guerrero, J.A. Ayllón, T. Calvet, M. Font-Bardia, J.G. Planas, J. Pons, Inorg. Chim. Acta 487 (2019) 295–306, https://doi.org/10.1016/j. ica.2018.12.025.

[42] W.-B. Shi, A.-L. Cui, H.-Z. Kou, CrystEngComm 16 (2014) 8027–8034, https://doi.org/10.1039/C4CE01082E.

[43] M.W. Njoroge, S.O. Ojwach, G.S. Nyamato, B. Omondi, J. Darkwa, J. Coord. Chem. 66 (2013) 1626–1634, https://doi.org/10.1080/00958972.2013.784904.

[44] W.L. Driessen, S. Gorter, W.G. Haanstra, L.J.J. Laarhoven, J. Reedijk, K. Goubitz, F. R. Selj´ee, Recl. Des Trav. Chim. Des Pays-Bas. 112 (2010) 309–313,

https://doi.org/10.1002/recl.19931120506.

[45] S. Tanase, E. Bouwman, G.J. Long, A.M. Shahin, R. De Gelder, A.M. Mills, A. L. Spek, J. Reedijk, Polyhedron 24 (2005) 41–48, https://doi.org/10.1016/j. poly.2004.07.026.

[46] L. Yang, D.R. Powell, R.P. Houser, J. Chem. Soc., Dalton Trans. (2007) 955–964, https://doi.org/10.1039/b617136b.

[47] A.W. Addison, T.N. Rao, J. Reedijk, J. van Rijn, G.C. Verschoor, J. Chem. Soc., Dalton Trans. (1984) 1349–1356, https://doi.org/10.1039/DT9840001349.

[48] R. Pothiraja, M. Sathiyendiran, A. Steiner, R. Murugavel, Inorg. Chim. Acta 372 (2011) 347–352, https://doi.org/10.1016/j.ica.2011.03.063.

[49] A.S. Potapov, E.A. Nudnova, G.A. Domina, L.N. Kirpotina, M.T. Quinn, A. I. Khlebnikov, I.A. Schepetkin, Dalton Trans. (2009) 4488–4498, https://doi.org/ 10.1039/b900869a.

[50] C. Di Nicola, A. Tombesi, M. Moroni, R. Vismara, F. Marchetti, R. Pettinari, L. Nardo, G. Vesco, S. Galli, S. Casassa, L. Pandolfo, C. Pettinari, CrystEngComm 22 (2020) 3294–3308, https://doi.org/10.1039/D0CE00370K.

[51] G. Esquius, J. Pons, R. Yáñez, J. Ros, X. Solans, M. Font-Bardia, Acta Crystallogr. Sect. C Cryst. Struct. Commun. 58 (2002) m133–m134, https://doi.org/10.1107/S0108270101020017.

[52] J. Pons, A. Chadghan, A. Alvarez-Larena, J. Francesc Piniella, J. Ros, Inorg. Chem. Commun. 4 (2001) 610–612, https://doi.org/10.1016/S1387-7003(01)00285-4.

[53] J. Pons, A. Chadghan, J. Casabo, A. Alvarez-Larena, J. Francesc Piniella, J. Ros, Inorg. Chem. Commun. 3 (2000) 296–299, https://doi.org/10.1016/S1387-7003(00)00073-3.

[54] J. Pons, X. López, E. Benet, J. Casabó, F. Teixidor, F.J. Sánchez, Polyhedron 9 (1990) 2839–2845, https://doi.org/10.1016/S0277-5387(00)84188-1.

[55] J. Casabó, J. Pons, K.S. Siddiqi, F. Teixidor, E. Molins, C. Miravitlles, J. Chem. Soc., Dalton Trans. 6 (1989) 1401–1403, https://doi.org/10.1039/DT9890001401.

[56] A.K. Das, A. De, P. Yadav, F. Lloret, R. Mukherjee, Polyhedron 171 (2019) 365–373, https://doi.org/10.1016/j.poly.2019.07.023.

[57] T.L. Hu, J.R. Li, C. Sen Liu, X.S. Shi, J.N. Zhou, X.H. Bu, J. Ribas, Inorg. Chem. 45 (2006) 162–173, https://doi.org/10.1021/ic051488d.

[58] X.B. Liu, D.H. Huan, G.H. Cui, L.H. Han, J. Struct. Chem. 56 (2015) 1124–1129, https://doi.org/10.1134/S0022476615060153.

[59] M.J. Hallam, C.A. Kilner, M.A. Halcrow, Acta Crystallogr. Sect. C Cryst. Struct. Commun. 58 (2002) 445–446, https://doi.org/10.1107/S010827010201154X.

[60] S. Roeser, S. Maji, J. Benet-Buchholz, J. Pons, A. Llobet, Eur. J. Inorg. Chem. 2013 (2013) 232–240, https://doi.org/10.1002/ejic.201200809.

[61] J.A. Perez, J. Pons, X. Solans, M. Font-Bardia, J. Ros, Inorg. Chim. Acta 358 (2005) 617–622, https://doi.org/10.1016/j.ica.2004.07.064.

[62] J. Pons, A. Chadghan, J. Casabó, A. Alvarez-Larena, J.F. Piniella, X. Solans, M. Font-Bardia, J. Ros, Polyhedron 20 (2001) 1029–1035, https://doi.org/ 10.1016/S0277-5387(01)00760-4.

[63] J. Pons, A. Chadghan, A. Alvarez-Larena, J.F. Piniella, J. Ros, Inorg. Chim. Acta 324 (2001) 342–346, https://doi.org/10.1016/S0020-1693(01)00566-7.

[64] A. Chadghan, J. Pons, A. Caubet, J. Casabó, J. Ros, A. Alvarez-Larena, J. Francesc Piniella, Polyhedron 19 (2000) 855–862, https://doi.org/10.1016/S0277-5387(00)00330-2.

[65] J. Pons, X. López, J. Casabó, F. Teixidor, A. Caubet, J. Rius, C. Miravitlles, Inorg. Chim. Acta 195 (1992) 61–66, https://doi.org/10.1016/S0020-1693(00)83850-5.

[66] B. Bleaney, K.D. Bowers, Proc. R. Soc. London. Ser. A. Math. Phys. Sci. 214 (1952) 451–465, https://doi.org/10.1098/rspa.1952.0181.

[67] L. Merz, W. Haase, J. Chem. Soc., Dalton Trans. 74 (1980) 875–879, https://doi. org/10.1039/dt9800000875.

[68] Y. Akhriff, J. Server-Carrió, A. Sancho, J. García-Lozano, E. Escrivá, J.V. Folgado, L. Soto, Inorg. Chem. 38 (1999) 1174–1185, https://doi.org/10.1021/ic980982x.

[69] T. Chattopadhyay, K.S. Banu, A. Banerjee, J. Ribas, A. Majee, M. Nethaji, D. Das, J. Mol. Struct. 833 (2007) 13–22, https://doi.org/10.1016/j. molstruc.2006.08.024.

[70] P. Sepp¨ala¨, E. Colacio, A.J. Mota, R. Sillanp¨aa¨, Inorg. Chim. Acta 363 (2010) 755–762, https://doi.org/10.1016/j.ica.2009.11.035.

[71] V.H. Crawford, H.W. Richardson, J.R. Wasson, D.J. Hodgson, W.E. Hatfield, Inorg. Chem. 15 (1976) 2107–2110, https://doi.org/10.1021/ic50163a019.

[72] E. Ruiz, P. Alemany, S. Alvarez, J. Cano, Inorg. Chem. 36 (1997) 3683–3688, https://doi.org/10.1021/ic970310r.

[73] E. Ruiz, P. Alemany, S. Alvarez, J. Cano, J. Am. Chem. Soc. 119 (1997) 1297–1303, https://doi.org/10.1021/ja961199b.

[74] H. Hu, D. Zhang, Z. Chen, C. Liu, Chem. Phys. Lett. 329 (2000) 255–260, https://doi.org/10.1016/S0009-2614(00)01015-0.

[75] G.A. Bain, J.F. Berry, J. Chem. Educ. 85 (2008) 532, https://doi.org/10.1021/ ed085p532.

[76] G.M. Sheldrick, Acta Crystallogr. Sect. C Struct. Chem. 71 (2015) 3–8, https://doi.org/10.1107/S2053229614024218.

[77] C.F. Macrae, P.R. Edgington, P. McCabe, E. Pidcock, G.P. Shields, R. Taylor, M. Towler, J. van de Streek, J. Appl. Crystallogr. 39 (2006) 453–457, https://doiorg/10.1107/S002188980600731X.

[78] C.F. Macrae, I.J. Bruno, J.A. Chisholm, P.R. Edgington, P. McCabe, E. Pidcock, L. Rodriguez-Monge, R. Taylor, J. van de Streek, P.A. Wood, J. Appl. Crystallogr. 41 (2008) 466–470, https://doi.org/10.1107/S0021889807067908.

[79] C. Cason, T. Froehlich, C. Lipka, POV-Ray for Windows, Persistence of Vision Raytracer Pty, Persistence Vis. Pty. Ltd., Williamstown, Victoria, Aust. (Version 3.7). (2013).

694 **Table 1**. Selected bond lengths (Å), angles (◦) and intermolecular hydrogen bond parameters
695 of 1.

696

Bond lengths (Å)			
Cu(1)-O(1)	1.9391(17)	Cu(2)-O(1)	1.8958(16)
Cu(1)-O(2)	1.9686(17)	Cu(2)-O(2)	1.9062(17)
Cu(1)-Cl(2)	2.2230(8)	Cu(1)-N(3)	1.945(2)
Cu(1)-Cl(1)	2.2397(7)	Cu(1)-N(1)	1.961(1)
Cu(1)···Cu(2)	2.9630(5)		
Bond angles (°)			
O(1)-Cu(1)-O(2)	76.09(7)	O(1)-Cu(2)-O(2)	78.61(7)
O(1)-Cu(1)-Cl(2)	168.11(5)	O(1)-Cu(2)-N(3)	156.68(9)
O(2)-Cu(1)-Cl(2)	94.77(5)	O(2)-Cu(2)-N(3)	91.23(8)
O(1)-Cu(1)-Cl(1)	92.80(5)	O(1)-Cu(2)-N(1)	94.23(8)
O(2)-Cu(1)-Cl(1)	161.49(6)	O(2)-Cu(2)-N(1)	165.39(8)
Cl(2)-Cu(1)-Cl(1)	97.93(3)	N(3)-Cu(2)-N(1)	99.84(9)

Intermolecular Hydrogen Bond Parameters				
	D-H (Å)	H···A (Å)	D···A (Å)	<D-H···A (°)
C5-H5···Cl2	0.950	2.688	3.636	175.47
C8-H8···O5	0.950	2.416	3.276	150.52
C32-H32··· O5	0.950	2.527	3.168	124.94
#1: -x + 1, y, -z + 1/2				

697

698

699

700

701

702

703

704

Table 2. Selected bond lengths (Å), angles (◦) and intermolecular hydrogen bond parameters for 2.

Bond lengths (Å)			
Cu(1)-N(2)	1.9805(8)	Cu(1)-Cl(1)	2.2322(3)
Cu(1)-O(1)	1.9985(8)	Cu(1)-Cl(2)	2.4818(4)
Cu(1)-N(1)	2.0261(9)		
Bond angles (°)			
N(2)-Cu(1)-O(1)	87.45(3)	N(1)-Cu(1)-Cl(1)	97.06(3)
N(2)-Cu(1)-N(1)	79.50(3)	N(2)-Cu(1)-Cl(2)	101.03(3)
N(1)-Cu(1)-O(1)	166.79(3)	Cl(2)-Cu(1)-O(1)	90.88(2)
N(2)-Cu(1)-Cl(1)	153.75(3)	N(1)-Cu(1)-Cl(2)	93.60(3)
O(1)-Cu(1)-Cl(1)	93.74(2)	Cl(1)-Cu(1)-Cl(2)	105.162(11)
N(3)-Cu(1)-O(1)	89.27(4)	N(3)-Cu(1)-O(5)	100.27(6)

Intermolecular Hydrogen Bond Parameters				
	D-H (Å)	H···A (Å)	D···A (Å)	<D-H···A (°)
O1-H1O···O1W	0.840	1.801	2.624	166.08
O1W-H1WA···Cl2	0.796	2.435	3.215	166.39
O1W-H1WB···Cl2	0.804	2.309	3.111	175.82

716 **Table 3**. Selected bond lengths (Å), angles (◦) and intermolecular hydrogen bond parameters
717 for 3.

718

Bond lengths (Å)			
Cu(1)-O(1)	1.9008(10)	Cu(1)-N(3)	2.0251(11)
Cu(1)-O(1)#1	1.9501(10)	Cu(1)-N(1)	1.9505(11)
Cu(1)-O(3)	2.474(1)	Cu(1)···Cu(1)#1	3.0408(4)
Bond angles (°)			
O(1)-Cu(1)-O(1)#1	75.70(5)	O(1)-Cu(1)-N(1)	169.46(5)
O(1)#1-Cu(1)-N(1)	94.38(4)	O(1)-Cu(1)-N(3)	93.27(4)
O(1)#1-Cu(1)-N(3)	160.89(5)	N(1)-Cu(1)-N(3)	95.27(5)
O(1)-Cu(1)-O(3)	87.74(4)	O(1)#1-Cu(1)-O(3)	94.40(4)
N(1)-Cu(1)-O(3)	96.65(5)	N(3)-Cu(1)-O(3)	100.81(5)
Intermolecular Hydrogen Bond Parameters			
	D-H (Å)	H···A (Å)	D···A (Å)	<D-H···A (°)
C8-H8···O2	0.950	2.531	3.420	155.83
C31-H31A···N6	0.990	2.622	3.413	136.92
C33-H33C··· O2	0.980	2.599	3.464	147.17
C12-H12···Cg1[a]	0.950	3.535	4.153	124.99
[a]Cg1 = C10-C15; #1: -x + 1, y + 2, -z + 1				

719

720

721

722

723

724

725

726

727 **Table 4**. Selected bond lengths (Å), angles (◦) and intermolecular hydrogen bond parameters
728 for 4.

729

Bond lengths (Å)			
Cu(1)-N(3)	1.955(4)	Cu(1)-N(4)	2.097(5)
Cu(1)-N(2)	1.960(5)	Cu(1)-O(1)	2.207(4)
Cu(1)-N(1)	2.077(5)	Cu(1)···Cu(1)	4.0448(9)
Bond angles (°)			
N(3)-Cu(1)-N(2)	91.43(17)	N(2)-Cu(1)-N(1)	79.81(18)
N(3)-Cu(1)-N(1)	168.8(2)	N(3)-Cu(1)-N(4)	79.70(18)
N(2)-Cu(1)-N(4)	166.74(18)	N(1)-Cu(1)-N(4)	107.63(19)
N(3)-Cu(1)-O(1)	96.43(17)	N(2)-Cu(1)-O(1)	104.99(19)
N(1)-Cu(1)-O(1)	92.55(19)	N(4)-Cu(1)-O(1)	85.93(19)
Intermolecular Hydrogen Bond Parameters			
	D-H (Å)	H···A (Å)	D···A (Å)	<D-H···A (°)
O1-H1OA···O3	0.797	2.061	2.756	145.70
O1-H1OB···O7	0.815	1.917	2.724	170.88
O1W-H7OA···O7	0.811	2.080	2.566	118.33
#1: -x + 1/4, -y + 1/4, z				

730

731

732

733

734

735

736

737

738 **Table 5**. Crystallographic data for complexes 1–4.

739

	1	2B	3	4
Empirical Formula	$C_{85}H_{76}Cl_4Cu_4N_{10}O_5$	$C_{16}H_{18}Cl_4CuN_4O_2$	$C_{68}H_{60}Cu_2N_{12}O_8$	$C_{26}H_{24}Cu_2N_{10}O_9$
Formula weight	1713.51	503.68	1300.36	747.63
T (K)	100(2)	100(2)	100(2)	100(2)
Wavelength (Å)	0.71073	0.71073	0.71073	0.71073
System, space group	Monoclinic, *C2/c*	Triclinic, *P*-1	Triclinic, *P*-1	Orthorhombic, *Fddd*
Unit cell dimensions				
a (Å)	32.071(3)	7.1504(7)	9.8155(9)	18.360(2)
b (Å)	12.8910(12)	11.4516(10)	12.1884(12)	23.625(2)
c (Å)	21.3823(19)	13.4558(11)	13.9385(14)	27.038(3)
α (°)	90	115.148(3)	67.033(4)	90
β (°)	120.051(3)	94.615(3)	87.810(4)	90
ϒ (°)	90	93.934(3)	84.075(4)	90
V (Å^3)	7651.8(12)	987.66(15)	1527.1(3)	11728(2)
Z	4	2	1	16
D_{calc} (mg/m^3)	1.487	1.694	1.414	1.694
μ (mm^{-1})	1.297	1.667	0.764	1.523
F (000)	3520	510	674	6080
Crystal size (mm^{-3})	0.126*0.071* 0.046	0.348*0.158* 0.092	0.150*0.080* 0.060	0.120*0.090* 0.060
hkl ranges	$-40 \le h \le 40$, $-16 \le k \le 16$, $-26 \le l \le 26$	$-10 \le h \le 10$, $-16 \le k \le 16$, $-19 \le l \le 19$	$-13 \le h \le 14$–$17 \le k \le 17$–$19 \le l \le 19$	$-26 \le h \le 26$–$34 \le k \le 34$–$39 \le l \le 35$
2θ range (°)	2.475 to 26.541	3.082 to 30.620	2.086 to 30.549	2.290 to 31.063
Reflections collected/ unique /[R_{int}]	67,297 / 7851 / [R_{int}] = 0.0891	38,694 / 5964 / [R_{int}] = 0.0253	63778/ 9331 / [R_{int}] = 0.0355	70,856 / 4701 / [R_{int}] = 0.1015
Completeness to θ (%)	99.1	98.4	99.8	99.9
Absorption correction	Semi-empirical	Semi-empirical	Semi-empirical	Semi-empirical
Max. and min. transmission	0.7454 and 0.6969	0.7461 and 0.6694	0.7461 and 0.6980	0.7462 and 0.6972
Refinement method	Full-matrix least-square on F^2	Full-matrix least-square on F^2	Full-matrix least-square on F^2	Full-matrix least-square on F^2
Data/Restrains/Parameters	7851 / 7 / 501	5964 / 3 / 250	9331 / 0 / 407	4701 / 3 / 243
Goodness-on-fit on F^2	0.984	1.080	1.073	1.089
Final R indices [I > 2σ(I)]	$R_1 = 0.0358$ $wR_2 = 0.0878$	$R_1 = 0.0193$ $wR_2 = 0.0529$	$R_1 = 0.0331$ $wR_2 = 0.0805$	$R_1 = 0.0725$ $wR_2 = 0.1923$
R indices (all data)	$R_1 = 0.0583$ $wR_2 = 0.0972$	$R_1 = 0.0204$ $wR_2 = 0.0541$	$R_1 = 0.0405$ $wR_2 = 0.0872$	$R_1 = 0.1381$ $wR_2 = 0.2630$
Extinction coefficient	n/a	n/a	n/a	0.00051(10)
Largest diff. peak and hole (e.Å^{-3})	1.512 and −0.472	0.460 and −0.399	1.694 and −0.565	1.227 and −0.786

740

741

742

743

744

745

746

747

Figures Captions

Scheme 1. Representation of the reactions carried out in this work. Occluded solvent molecules have been excluded for clarity. 3,5-hdppz = 3,5-diphenylpyrazole; 3,5-dpypz = 3,5-(2-pyridyl)pyrazolate.

Figure 1. a) Complex 1, showing relevant atoms and their numbering scheme. Occluded solvent molecules have been excluded for clarity b) Supramolecular packing in 1, view along b axis. Occluded HL1 molecules are highlighted in blue. Detail of the association between dimeric units. c) Voids representation (1543.8 Å3, 20.2% of unit cell volume), view along c axis.

Figure. 2 a) Complex 2B, showing all its relevant atoms and numbering scheme. b) Supramolecular chains, view along c axis. c) Clathrate-like structure, view along a axis.

Figure 3. Complex 3, showing relevant atoms and their numbering scheme. Occluded solvent molecules have been excluded for clarity.

Figure 4. a) Supramolecular chains in 3, view along b axis. b) Interactions between chains along c axis (left) and a axis (right). Occluded CH3CN molecules are highlighted in green. Only relevant hydrogen atoms are shown.

Figure 5. a) Dimeric cation of complex 4, showing relevant atoms and numbering scheme. Occluded solvent molecules have been excluded for clarity. b) Supramolecular packing, showing all non-hydrogen atoms. Water molecules are highlighted in blue and space fill mode. View along a axis. c) Detail of the π-π stacking interactions.

Figure 6. Thermal variation of χpara for 3. Inset: thermal variation of χM for 3.Solid line represents best fit to the proposed model (see text)..

Scheme 1.

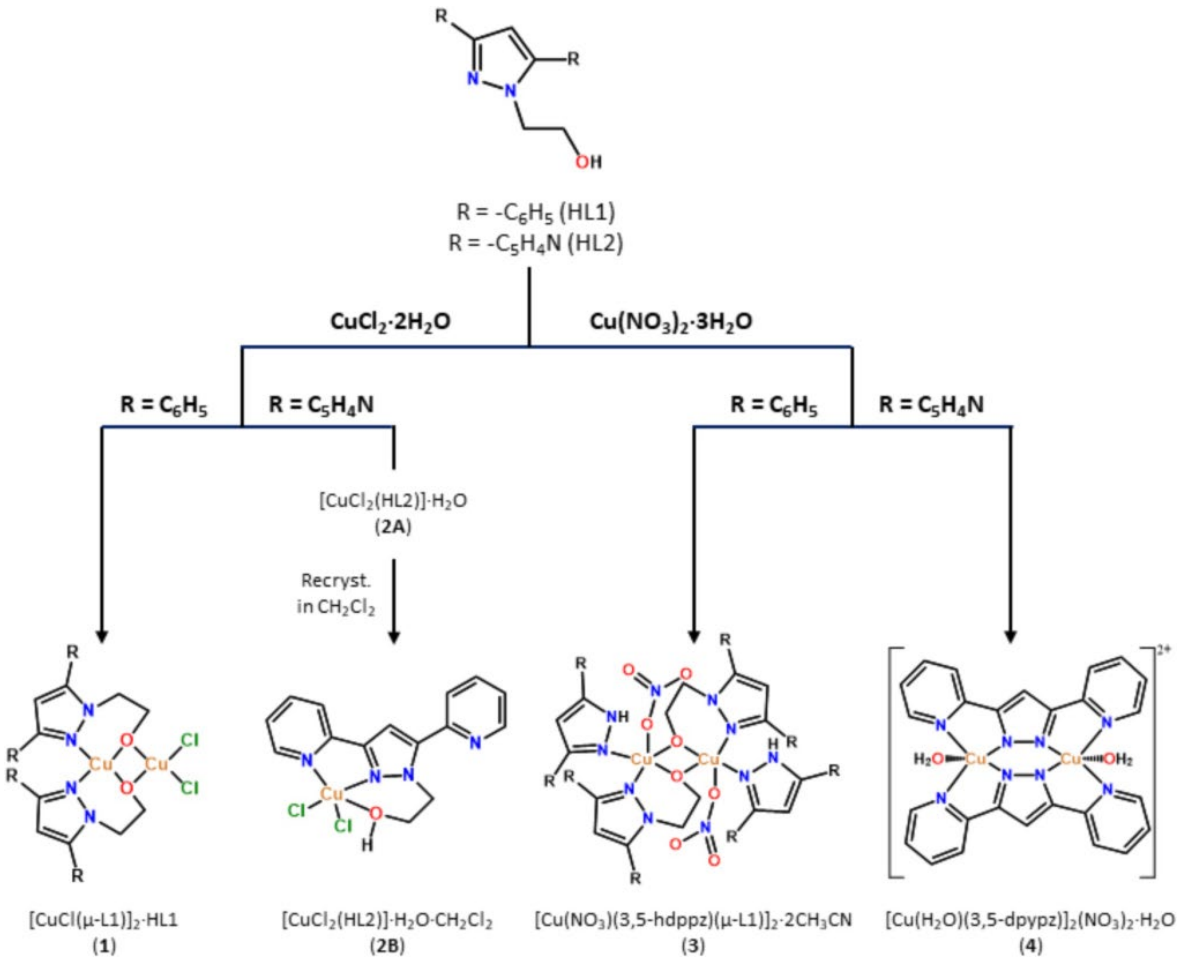
R = -C6H5 (HL1)
R = -C5H4N (HL2)
CuCl2·2H2O
Cu(NO3)2·3H2O
R = C6H5
R = C5H4N
R = C6H5
R = C5H4N
[CuCl2(HL2)]·H2O
(2A)
Recryst.
in CH2Cl2
[CuCl(μ-L1)]2·HL1
(1)
[CuCl2(HL2)]·H2O·CH2Cl2
(2B)
[Cu(NO3)(3,5-hdppz)(μ-L1)]2·2CH3CN
(3)
[Cu(H2O)(3,5-dpypz)]2(NO3)2·H2O
(4)

Figure 1

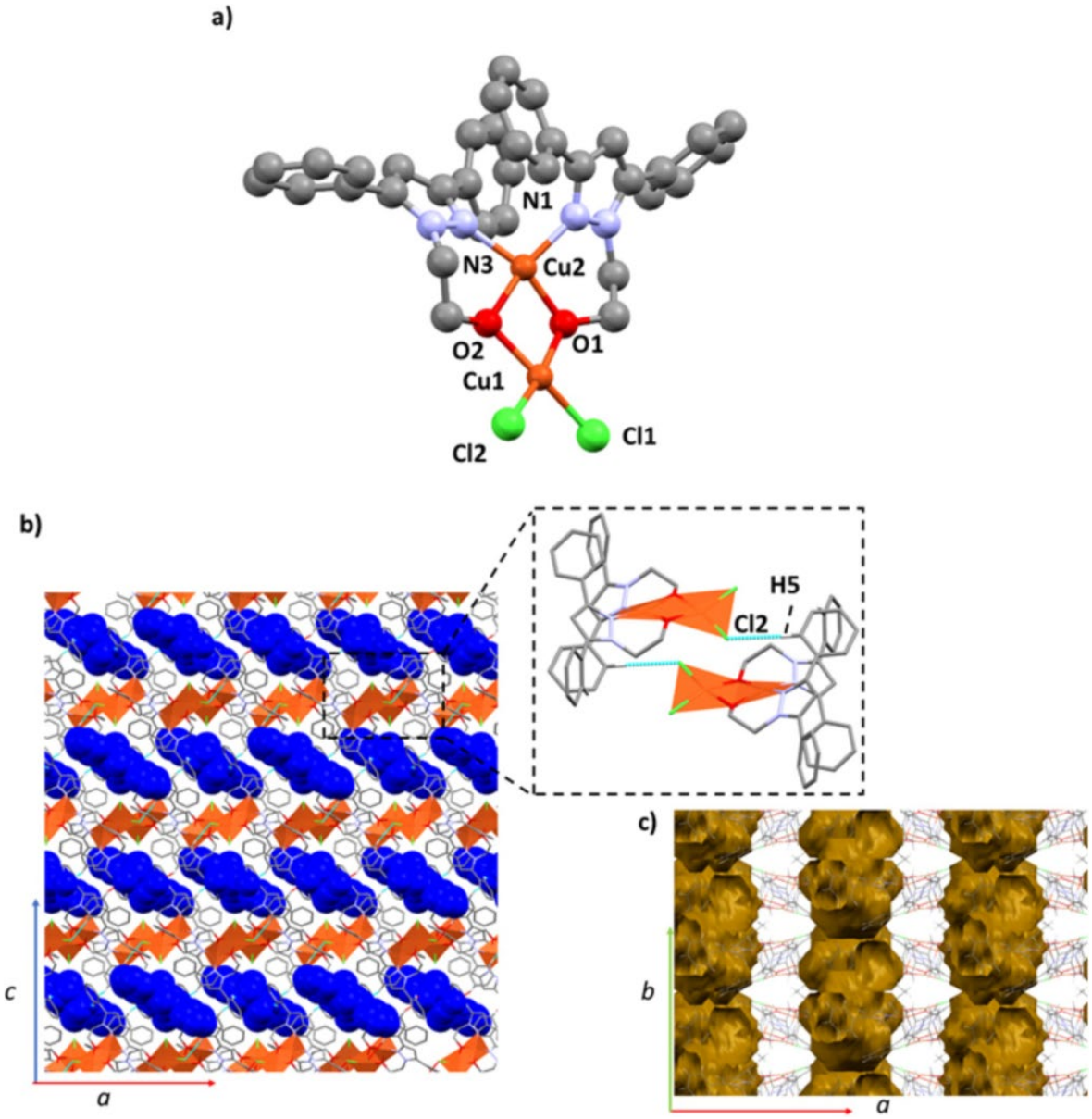

Figure 2

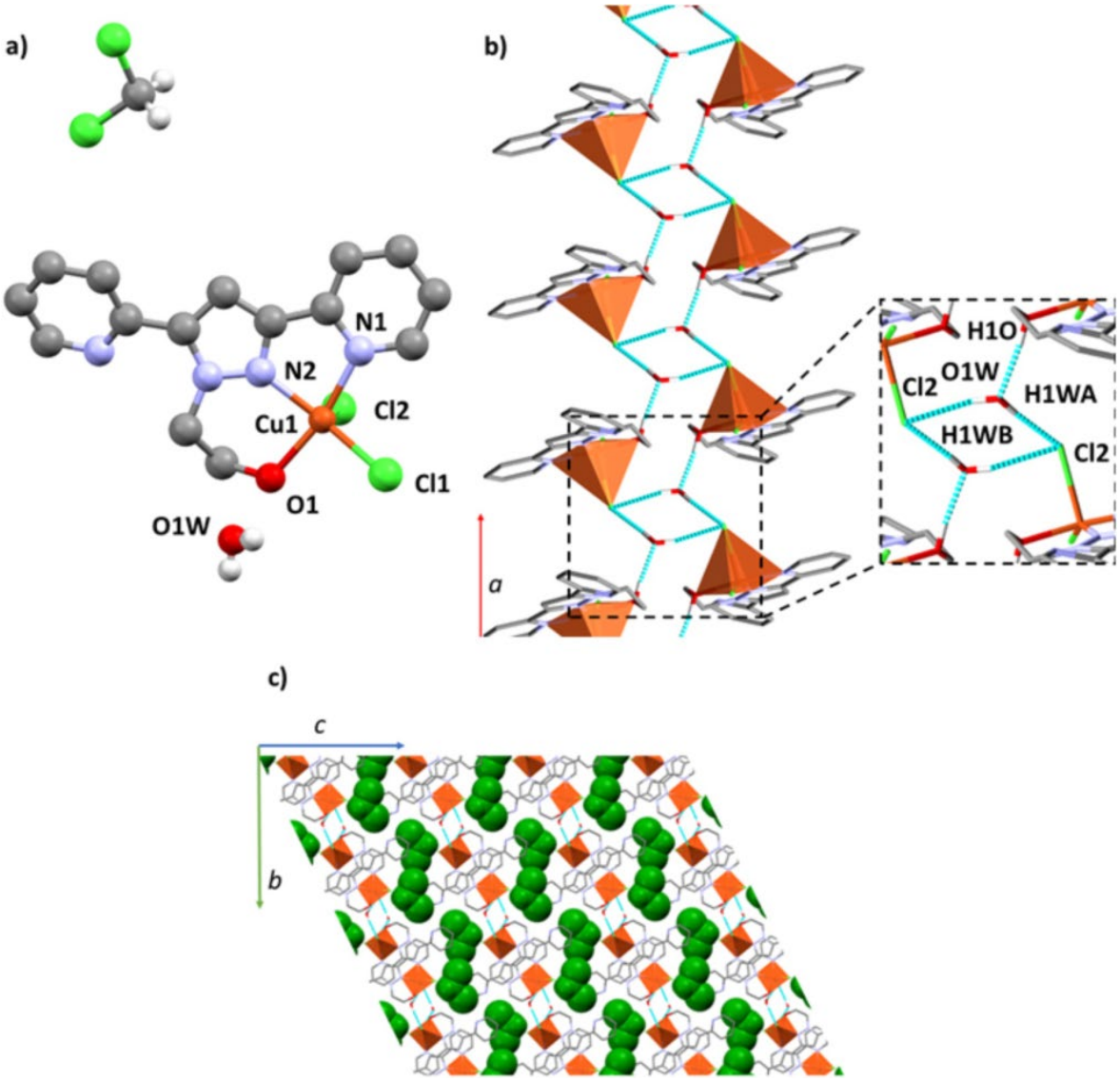

Figure 3

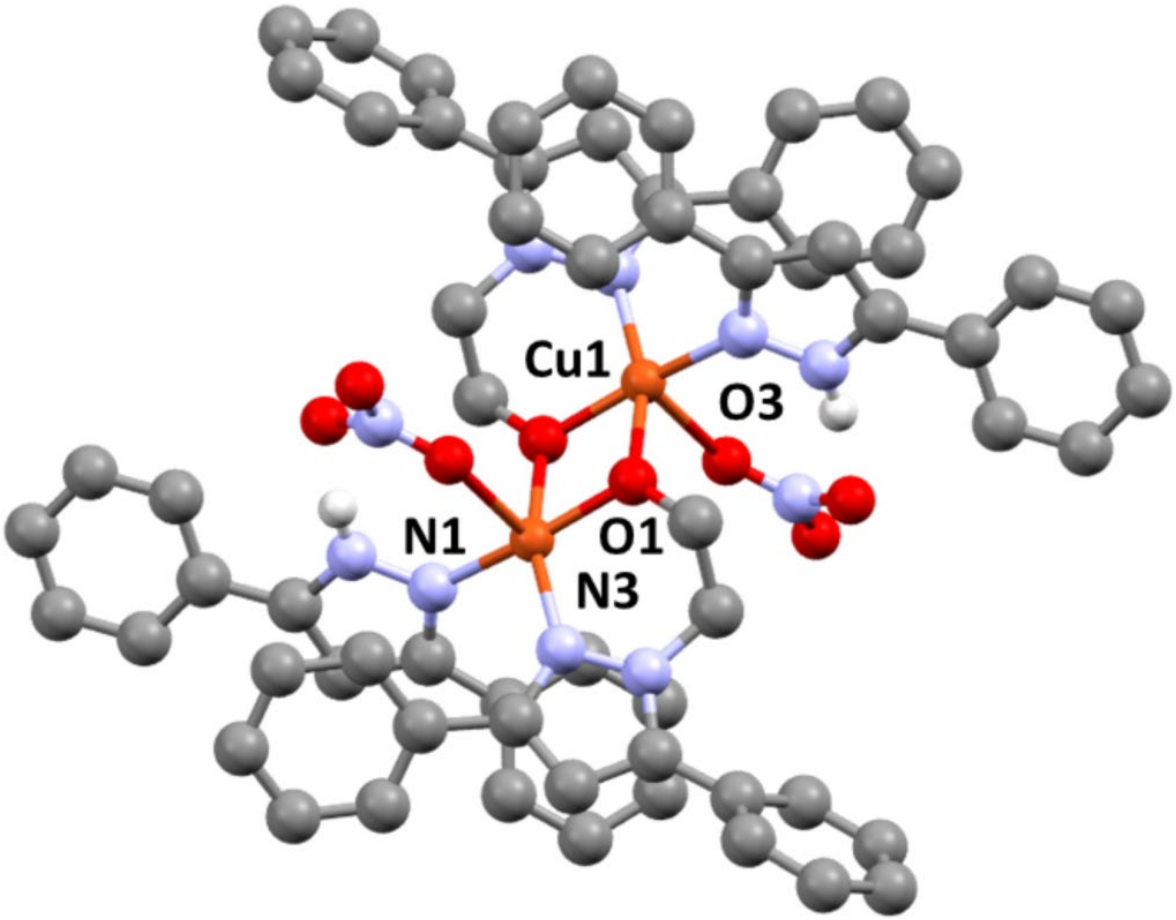

Figure 4

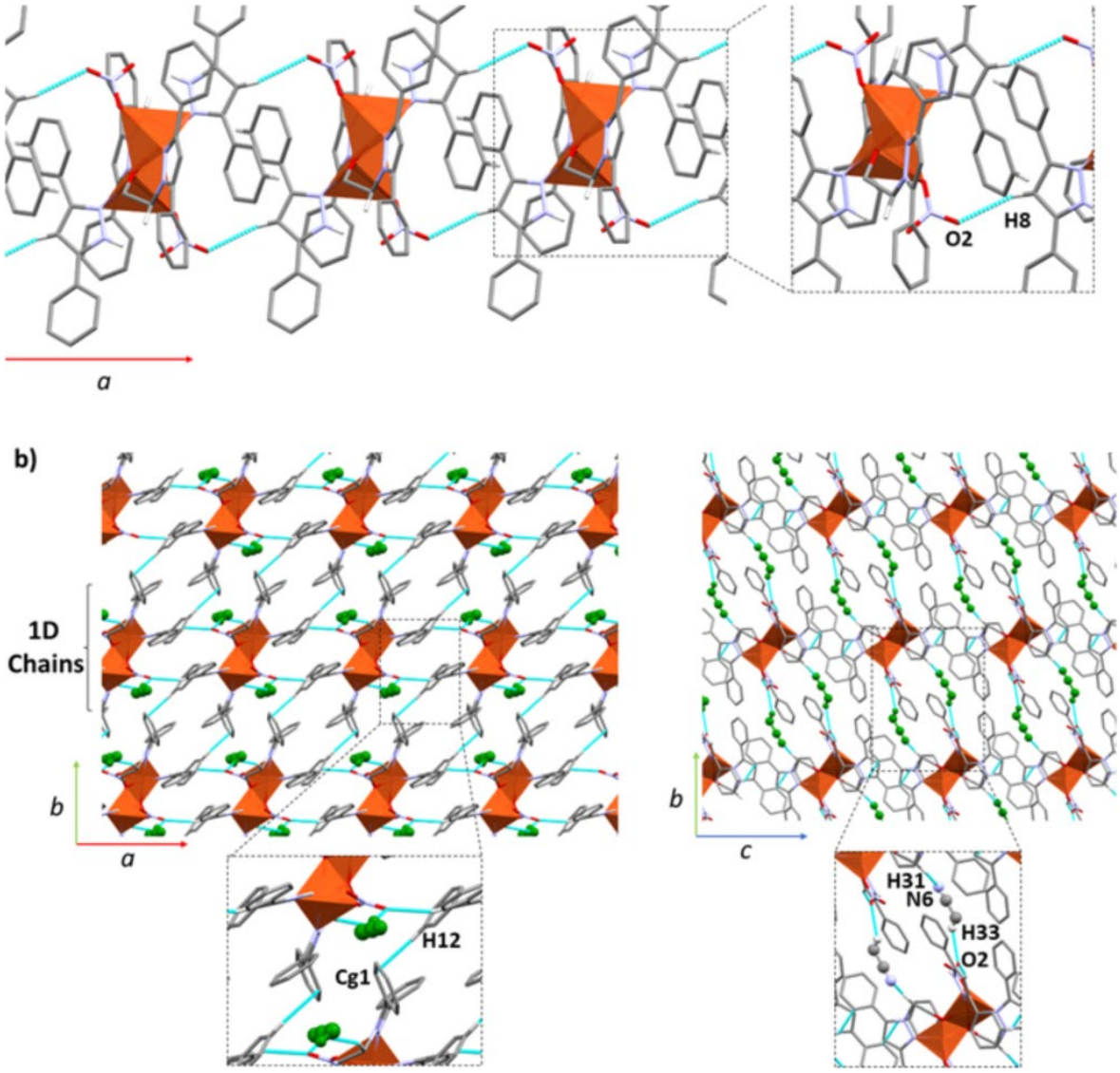

Figure 5

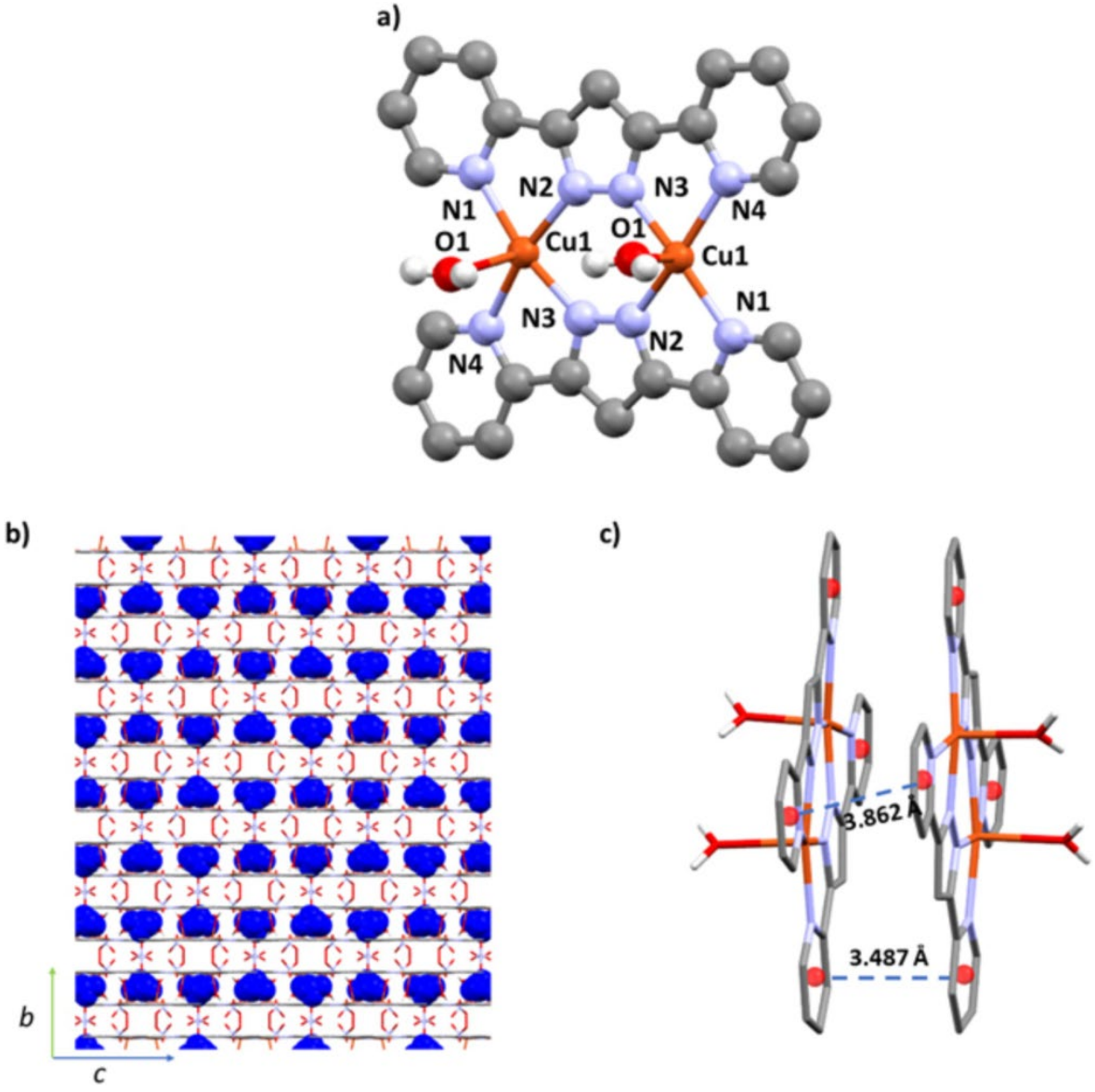

Figure 6

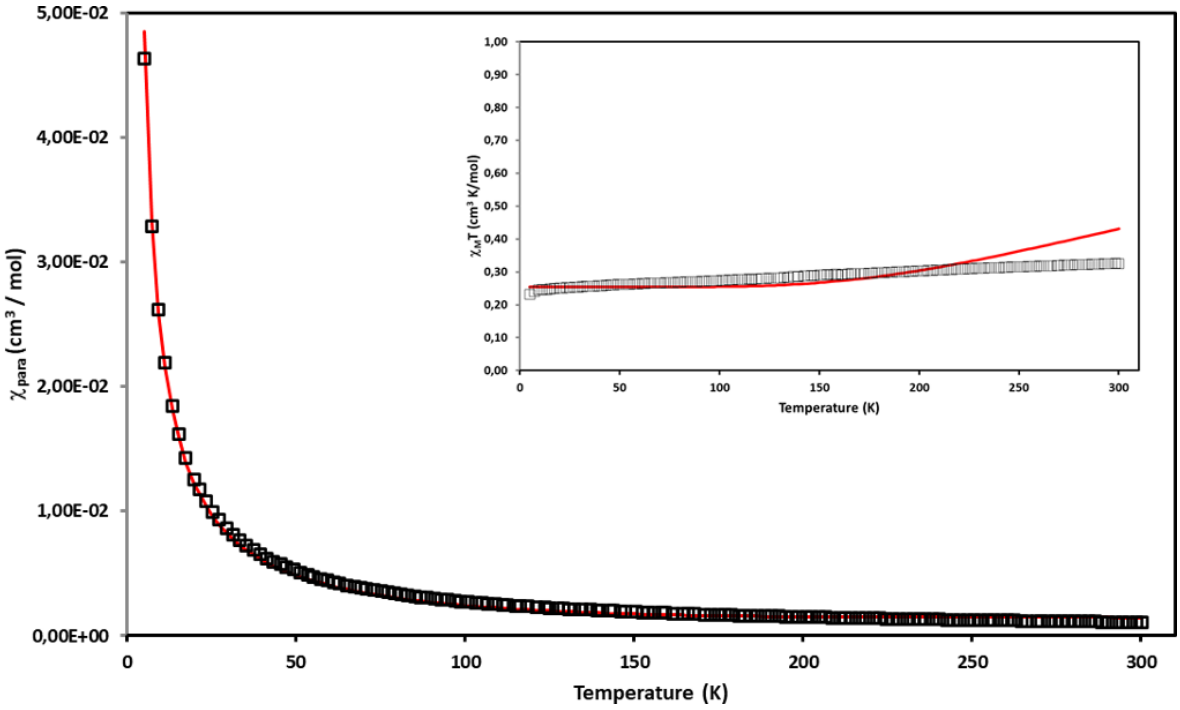
5,00E-02
4,00E-02
3,00E-02
2,00E-02
1,00E-02
0,00E+00
χpara (cm³ / mol)
0
50
100
150
200
250
300
Temperature (K)
1,00
0,90
0,80
0,70
0,60
0,50
0,40
0,30
0,20
0,10
0,00
χMT (cm³ K/mol)
0
50
100
150
200
250
300
Temperature (K)